Nonlinear Force Control of Dielectric Electroactive Polymer Actuators

Muzaffer Y. Ozsecen and Constantinos Mavroidis[1]

Department of Mechanical and Industrial Engineering, Northeastern University
360 Huntington Avenue, Boston MA 02115

ABSTRACT

Electroactive Polymers (EAPs) have a great potential to provide smart solutions to engineering problems in fields such as robotics, medical devices, power generation, actuators and sensors. This is because they yield some important characteristics that are advantageous over conventional types of actuators, like: lower weight, faster response, higher power density and quieter operation. Controlling the amount of force exerted during an interaction between an actuator and an object is crucial for certain applications, such as those involving a human and an actuator. To date there is little research into the force control of EAPs or their possible applications that utilize force control. This paper presents a real-time nonlinear force controller for a Rolled type Dielectric Electroactive Polymer Actuator (DEA). To increase the response of the actuator, a control algorithm and an inverse model were derived using the actuator's nonlinear behavior. The force controller presented can enhance the safety and performance of this unique family of actuators, allowing for more advanced and efficient applications.

Keywords: Dielectric Elastomers, Electro-Active Polymer Actuators, Nonlinear Control.

1. INTRODUCTION

Dielectric Electroactive Polymer Actuators (DEAs) are able to combine actuation, sensing and structure in a single material. They operate with high power density and unlike conventional actuators, do not encounter friction problems at low speeds. Electric motors, pneumatic, and hydraulic systems are types of conventional actuators that are used frequently in industrial applications and robotics due to accomplishments of control over these actuators [1]. On the other hand, the increasing interest in the field of EAPs is resulting in development of new types of actuators. Dielectric elastomers have been previously implemented as rolls, tubes, stacks, diaphragms, extenders, folded, bimorph and unimorph [2]. DEAs are very unique and functional since they combine large active deformations, high energy densities, good efficiencies and fast response compared to other Electric EAPs. These characteristics enable designers and engineers to form new principles of actuation types and processes according to society needs. In order to provide solutions to society's needs that take advantage of EAP technology, control of this unique family of actuators could be considered as a parallel path to be proceeded to utilize electroactive polymer systems in the future. Compared to electromagnetic motors and linear actuators DEAs have greater power density efficiency at lower operational speeds since gearing is eliminated. The material and production costs are estimated to be lower than electromagnetic actuators and they come in greater size and shape variations [3]. DEAs have promising aspects for many applications in the fields of: consumer electronics, medical instruments, MEMS, biomimetics, robotics and haptics, since they can be manufactured for custom applications.

Dielectric EAP actuators are also referred as Dielectric Elastomer Actuators, and fall in the category of Electric EAPs (see Figure 1 for classification of EAP materials). Response of the electroactive film is the result of electrostatic charge on the electrodes. When charged with opposite polarity, the electrodes attract each other creating pressure (ρ) on the film. The volume remains constant, so as the film thickness decreases, the surface area increases. In a rolled type DEA actuator for example the generated pressure results in a linear motion since the film is constrained on both sides. When the voltage is switched off, the DEA contracts back to its original shape. The electromechanical model that describes the pressure exerted on the silicon layer ρ is [4-6] :

$$\rho = \epsilon_r \epsilon_o E^2 = \epsilon_r \epsilon_o \left(\frac{V}{t}\right)^2 \tag{1}$$

[1] Professor-Corresponding Author, Tel: 617-373-4121, Fax: 617-373-2921, Email: mavro@coe.neu.edu,
Webpage: http://www.coe.neu.edu/~mavro

Electroactive Polymer Actuators and Devices (EAPAD) 2010, edited by Yoseph Bar-Cohen,
Proc. of SPIE Vol. 7642, 76422C · © 2010 SPIE · CCC code: 0277-786X/10/$18 · doi: 10.1117/12.847240

Where ϵ_0 and ϵ_r are the permittivity of free space and the relative permittivity of the polymer; E is the applied electric field; V is the voltage and t is the film thickness. Pressure on the film creates the force along the direction of elongation and it is directly proportional to the square of voltage. As can be seen from Equation 1, a nonlinear response of force is expected with varying voltage values.

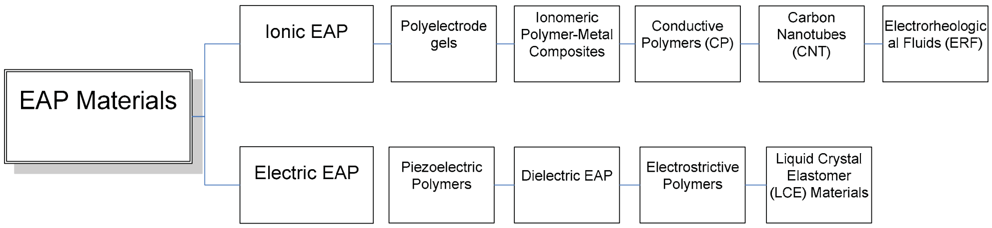

Figure 1: Classification of EAP Materials.

Experimental and mathematical characterization of electroactive polymers is still being developed. Fox and Goulbourne recently demonstrated electromechanical dynamic response of a DE membrane subject to pressure and reported the sensitivity of electrical loading on the membrane [7]. Huynh, Alici and Spinks worked on system identification and validation of their conductive polymer actuator model [8]. Material selection for Dielectric Elastomer Actuator changes the mechanical properties of the film and therefore the control structure has to be altered accordingly. It was observed that although different materials had been used as the building block, nonlinear behavior of DEAs of the actuators was consistent. Precise modeling and control was adapted to tackle difficulties caused by nonlinearity in many studies. In control studies conducted with Ionic Polymer Metal Composites (IPMCs) [1, 9-10] Richardson et.al. investigated the polymer performance with impedance control. Another feedback control method by Mallavarapu, Newbury and Leo used Linear Quadratic Regulator (LQR). Bhat and Kim further looked into hybrid force and position control strategy by implementing empirically obtained plant transfer function for precision control. On the other hand, conjugated and conducting polymer research is following a similar approach to improve performance by implementing closed loop control. Qi, Lu and Mattes demonstrated the importance of closed loop control for conducting polymer actuators. Later Fang, Tan and Alici demonstrated that robust adaptive control scheme requires less effort than of PID control [11-12]. Similar approach has taken place on the control of Dielectric Elastomer Actuators. Carpi and De Rossi experimentally validated their electromechanical model of a cylindrical actuator made of dielectric elastomer [2]. Toth and Goldenberg addressed the possible use of Dielectric Elastomer Transducers as a sensory subsystem and an actuator, hence by measuring strain and capacitance in real-time control [13]. Furthermore, Chuc et.al. studied the self-sensing capability of force in DE actuators [14]. Sarban, Oubaek and Jones introduced a closed-loop control of a core free rolled EAP actuator, same as the one used in this paper, using a gain scheduling algorithm with a PI controller [15]. Gisby, Calius, Xie and Anderson shared the results obtained from a control algorithm using PWM signals to control current [16].

To date little very little research has been conducted into the force control of EAP actuators or their possible applications which utilize force control such as haptics and human-robot interaction. In this paper we present, one of the first force controllers for EAP actuators utilizing a real-time nonlinear force control algorithm as this is applied on a Rolled type Dielectric Electroactive Polymer (RDEAP). To increase the response characteristics of the actuator, a control algorithm and non-linear inverse model were derived using the actuator's nonlinear behavior. Experiments have been conducted to compare the response of P, PI and PID controllers both with and without the feed forward non-linear term. A PID controller with the inverse model as a feed forward term has been found to give the fastest rising time (~40ms) and settling time (~50ms).

2. EXPERIMENTAL SYSTEM

To be able to experimentally compare various forces controllers for EAP actuators we have developed an experimental prototype composed of a linear DE actuator, a force sensor and a position sensor as shown in Figure 2. This prototype is essentially a 1 Degree of Freedom (DoF) platform, being able to move up and down using a InLastor-Push DE Actuator (DEA) manufactured by Danfoss PolyPower A/S. Actuator is capable of applying a maximum force of 6.7N. The maximum elongation was observed to be 1.3mm at 2.25kV. More information about the actuator could be reached from the company's website (http://www.polypower.com/Products/InLastor-Actuators.aspx). The prototype's structural elements (base, linkage) were fabricated using a Viper Stereolithography machine from 3D Systems Inc. A load cell (Honeywell 31 Mid series) is rigidly attached between the prototype's base and the DEA in order to obtain measurements for the forces applied by the DEA. A "median" linkage can move up and down based on the forces applied by the actuator under different payloads. A potentiometer (Active Sensor CLS1311), placed on the top of the prototype, measure's the distance and speed of the median linkage. Mechanical stops can fix the linkage at certain locations so that force control static experiments could be performed. The constructed test bed is 16cm wide and 35cm long. The maximum travel allowed for the median linkage is 5cm and the maximum payload capacity was designed to hold 2kg easy-grip test weight. The preloading was applied by test weights while being monitored by force sensor reading and fixed with mechanical stops.

The control hardware of the system consists of two PCs: a host computer, and a real-time target. The host computer runs LabVIEW that provides the Graphical User Interface and the communication with the real-time computer. The user can modify the experimental parameters through the GUI. Communication between the host and the real-time target is carried out by the LabVIEW Shared Variable Engine. The real-time target is the dedicated controller of the system that runs all the time critical tasks such as data acquisition and controls. For the implementation of the controller in the real time target computer, the LabVIEW graphical programming language running on a Real-Time Operating System (RTOS) has been used. The real-time target is equipped with a National Instruments 6259 M-Series I/O card. The digital controller implemented on the real-time target operates at a frequency of 5 kHz. The computer command signal to the actuator was amplified using a high voltage amplifier (TREK 609D-6). Figure 2 shows a close up view of the experimental prototype while Figure 3 shows all system electro-mechanical components.

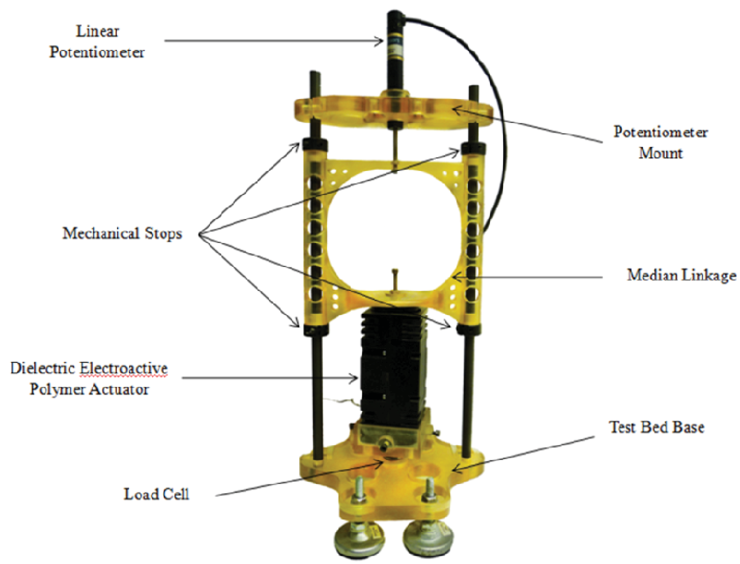

Figure 2: Test Bed Close-up View.

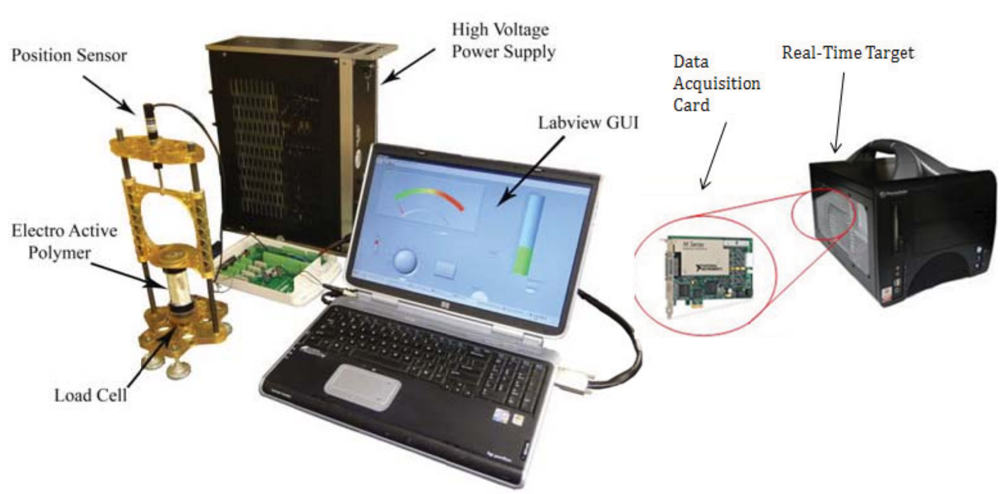

Figure 3: Experimental Test Bed.

3. INVERSE MODEL IDENTIFICATION

The non-linear force control algorithm presented in the next section is using a non-linear model in a feed-forward loop to take into account the DEA's non-linear behavior. This non-linear model calculates the voltage required to apply by the amplifier in order to develop a desired force by the actuator. We call it "inverse model" to make the distinction from the "direct" and most widely used model that calculates the force generated by the actuator when a voltage is applied. In this section we present the experimental identification procedures followed to calculate the "inverse model" of the DEA.

First we experimentally identified the "direct" model. Experiments were conducted via restraining the actuator's movement along the direction of motion using the mechanical stops and reading the force output using the compression load cell of the prototype. No preload was applied. A ramp input voltage was supplied with increments of 1V per 5ms, reaching up to 2250V in 11.25 seconds. The direct model (i.e. force-voltage relationship) thus obtained is shown in Figure 4.

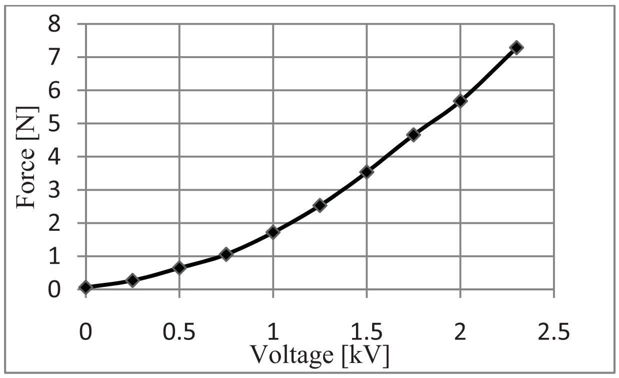

Figure 4: Blocked force measurement for DEA with no preload.

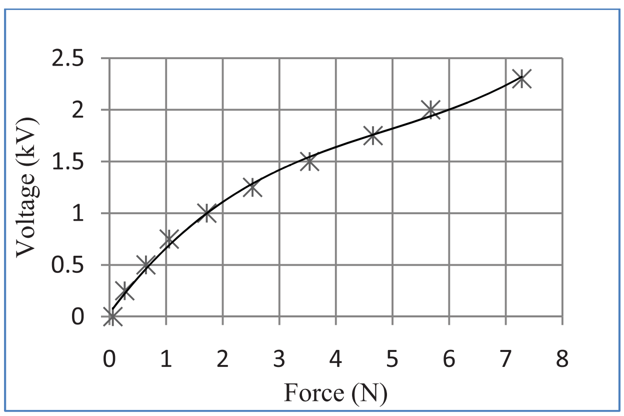

Figure 5: Inverse Model for DEA with average of multiple preloading conditions.

To calculate the inverse model and to eliminate any identification errors due to the actuator transient response a more thorough identification procedure was followed. A series of force measurements in steady state were collected under various step responses. Before starting the force measurements, noise in the setup was measured with respect to time and applied voltage signal. While force was continuously recorded at 5 kHz, the "median" linkage of the prototype while fixed using the mechanical stops was excited by a force generated by the DEA under a certain voltage value and then left to rest for a few seconds. Voltage was applied at the actuator as a step input of increments of 250V from 0 to 2.25kV. At every voltage level, the actuator's maximum force capability was recorded. The same voltage values were applied five times and the recorded forces were averaged to find the best approximation for every given preload condition. The averaged force measurements for every increment of voltage values were then put together to form the average step response curve for one preload condition. The same procedure was held for more preloading conditions starting from 0 to 18N with 2N increments. By averaging the best approximate values for every preloading condition (from 0N to 18 N); a final force-voltage curve was generated that accommodated each preloading condition as an average of load and condition size. Plotting the data as a voltage-force curve this time (i.e. inverting the model) the graph of Figure 5 was obtained where the stars indicate the experimentally measured data. A third degree polynomial was used to interpolate the data as shown in Equation 2:

$$v = 0.0078f^3 - 0.115f^2 + 0.7365f + 0.0327 \quad (2)$$

Open loop control experiments were conducted using the inverse model as shown in the block diagram of Figure 6. An example from these open loop control tests under a step input is shown in Figure 7. The system, even with no feedback, performs overall very well (relatively fast response with not a lot of overshoot). However, the system showed a steady state error of 24% that was due to uncertainties that were not taken into account in the model and this demonstrates the need for a closed loop control.

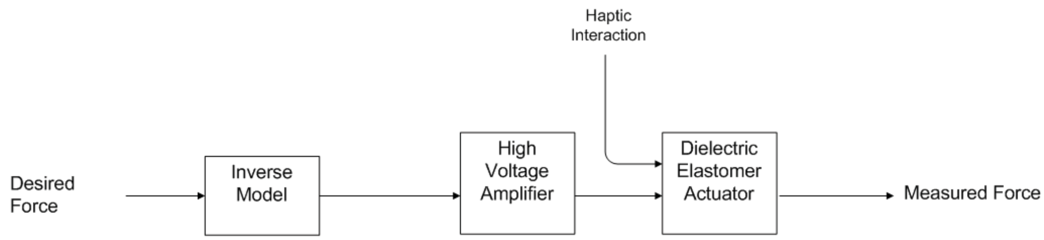

Figure 6: Open loop control structure of the system.

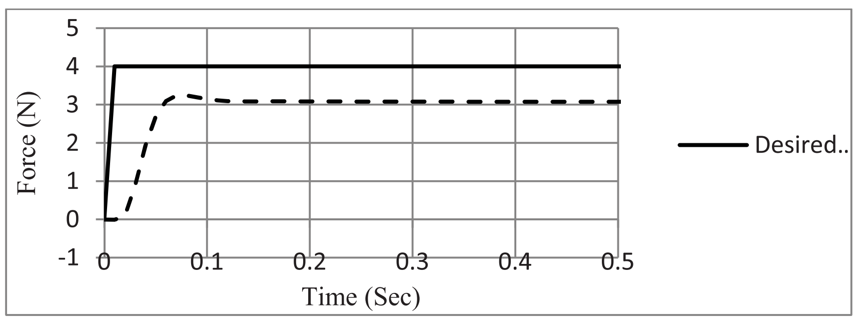

Figure 7: System response with feedforward term only.

4. CLOSED LOOP FORCE CONTROLLER

A schematic of the proposed non-linear closed loop force control algorithm for DE actuators is shown in Figure 8. The controller contains a feedback loop for the force to obtain the force error that will be processed by the controller and a feedforward loop that contains the inverse model whose output is added to the controller output. The Zeigler-Nichols PID control tuning method was adopted to identify the control gains [17]. The gain parameters were even further fine-tuned later in order to achieve fast transient response with less than 5% overshoot and no steady state error.

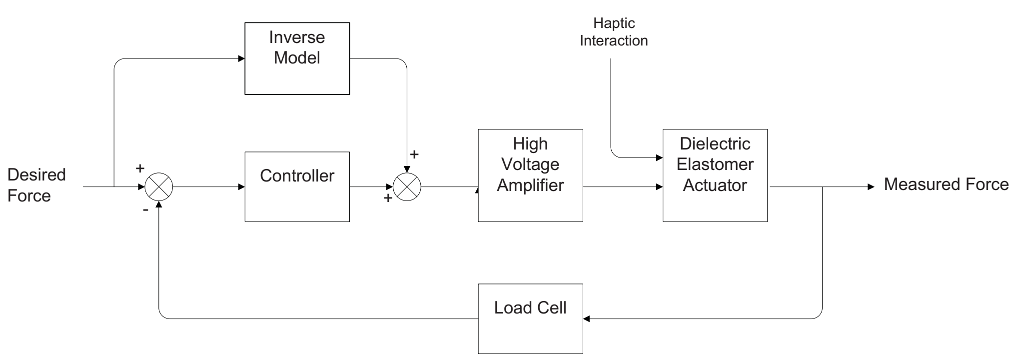

Figure 8: Closed loop control structure of the system.

The Graphical User Interface that was used for parameter selection during the controller tuning is shown in Figure 9. The GUI consisted of an input/output force graph and displays the numeric rise time, the settling time and overshoot of the streamed data. The user was able to select the type of desired input signal from a list consisting of step, ramp, sinusoidal and square functions and entered the desired signal amplitudes and frequencies. Gauge types of displays were used to show the voltage requirements of each gain in the controller so that the user can see the amount of voltage drawn by the controller gain immediately after a change.

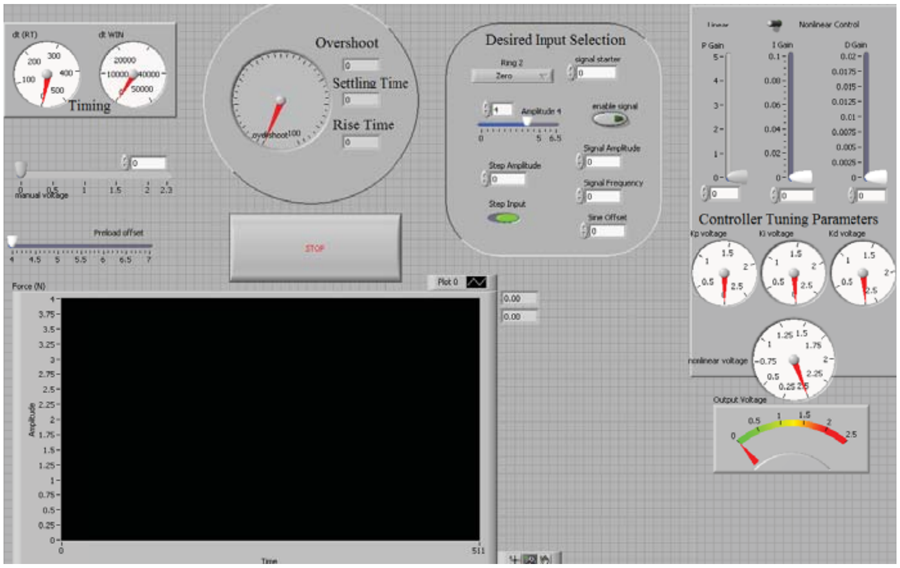

Figure 9: Graphical User Interface for controller development and experiments.

We performed various experiments using different controllers and we compared them. Below, when we refer to non-linear P, PI or PID control we mean that a feedfoward loop with the inverse model is included in the control algorithm as shown in Figure 8, while we refer to linear P, PI or PID control when the feedforward loop is not included. Initially, open loop control experiments with the nonlinear feed forward term showed a steady state error of 24%. Therefore a P controller was implemented (i.e. non-linear P). After tuning the proportional gain Kp, a 4.35% steady state error was observed with a 0.19 seconds settling time and 19% overshoot. Then, to compensate for the steady state error an integral term was introduced, (i.e. non-linear PI controller). In this case the steady state performance improved up to 0.5% steady state error with 0.13 seconds settling time and an overshoot of 22.3%. To compensate for the overshoot this time a derivative term was added and the resulting non-linear PID controller had 0.1% steady state error with 0.05 seconds settling time and only 1.18% overshoot.

We then studied the performance of the linear P, PI and PID controllers. The linear P controller had a 30% steady state error, which was 25.65% higher than the nonlinear P controller. It also had a 3.5% overshoot which was 15.5% lower than the nonlinear P controller. The linear PI controller was then introduced, that had a 23.6% overshoot with 0.13 seconds of settling time and a steady state error of 0.01%. The steady state performance was improved compared to the nonlinear PI controller while the transient responses of the linear and nonlinear PIs were very similar for both the linear and non-linear PI. The linear PID controller had no overshoot, the settling time was 0.05 seconds and the steady state error was less than 0.01%. The comparison of the PID controllers with and without the feed forward term in a representative step response is shown in Figure 10.

Similar comparison for sinusoidal and triangular response tests is shown in Figures 11 and 12 respectively. In both periodic input tests, frequencies of 1, 2, 5 and 10 Hz were selected to cover frequencies that are relatively close to human haptic perception levels. For the 1 Hz frequency of sine wave the linear PID lead the desired input showing an error in following the desired trajectory while the nonlinear PID controller followed it very accurately as shown in Figure 11. In sine inputs of 2 Hz both controllers performed similarly. Looking at the 5 and 10 Hz sine inputs the linear PID starts leading after 2.0 seconds where as nonlinear PID shows a minor lag. Similar results were observed with the triangular wave input tests as shown in Figure 12. At all frequencies the linear PID showed a clear lead from the desired signal whereas the nonlinear PID had a better performance than linear one.

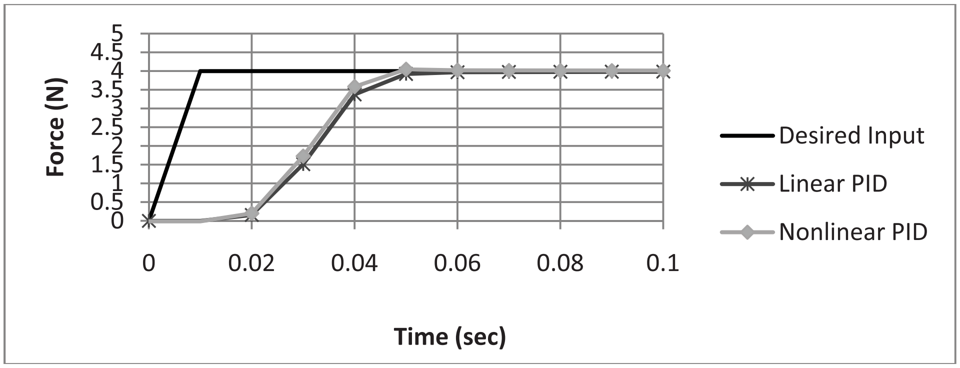

Figure 9: Comparison of controllers

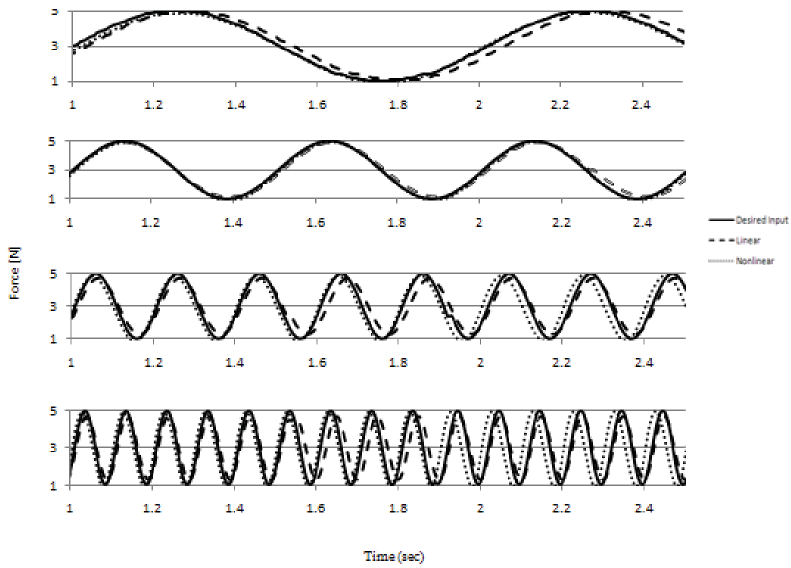

Figure 11: Linear/Nonlinear PID Controller close loop response to Sinusoidal input. Amplitude: 4N, Frequencies: 1, 2, 5, 10 Hz.

5. CONCLUSIONS

Controlled interaction between an actuator and its environment is crucial in certain applications, such as those involving a human and an actuated device. Many applications in medicine, robotics and haptics fall into this category and in such cases controlling the interaction force is very important. Dielectric Elastomer Actuators due to their small size, flexible shape and noiseless operation are good candidates for being used as actuators in medical, haptic and robotic devices that interact with a human. In such cases, force control of DEA will be a necessity. To date there has been very little research regarding the force control of DEAs. In this paper we tried to bridge this gap by presenting a nonlinear PID force controller for DEAs. Performance comparison between nonlinear and linear P, PI and PID force controllers was conducted for various inputs such as step, sinusoidal and triangular. It was observed that the non-linear P and PI controllers were better than the linear ones while the linear and non-linear PID had a similar performance. However, in periodic inputs such as sine and triangular waves the non-linear PID control was better in following the desired force trajectory in comparison with the linear one that showed errors due to substantial leading.

ACKNOWLEDGEMENTS

The authors would like to thank Danfoss PolyPower A/S of Denmark (http://www.polypower.com/) for providing the DE actuator samples and for their technical support regarding the Dielectric Electroactive Polymer Technology.

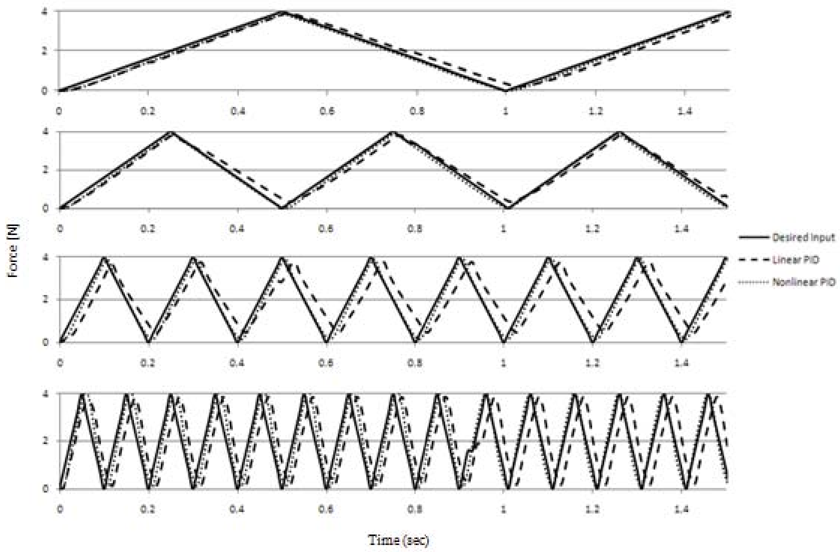

Figure 12: Linear/Nonlinear PID Controller close loop response to Ramp input. Amplitude: 4N, Frequencies: 1,2,5,10 Hz accordingly.

REFERENCES

[1] R. Richardson, M. Levesley, M. Brown *et al.*, "Control of ionic polymer metal composites", IEEE/ASME transactions on mechatronics*,* 8(2), 245-253 (2003).

[2] F. Carpi, and D. De Rossi, "Dielectric elastomer cylindrical actuators: electromechanical modelling and experimental evaluation", Materials Science & Engineering C*,* 24(4), 555-562 (2004).

[3] Y. Bar-Cohen, [Electroactive polymer (EAP) actuators as artificial muscles: reality, potential, and challenges], The Society of Photo-Optical Instrumentation Engineers, Bellingham, 529-577 (2004).

[4] R. Pelrine, R. Kornbluh, and J. Joseph, "Electrostriction of polymer dielectrics with compliant electrodes as a means of actuation", Sensors & Actuators: A. Physical*,* 64(1), 77-85 (1998).

[5] M. Wissler, E. Mazza, and G. Kovacs, "Circular pre-strained dielectric elastomer actuator: modeling, simulation and experimental verification", Proc. SPIE 5759, 182 (2005).

[6] R. Sarban, J. Oubaek, and R. Jones, "Closed-loop control of a core free rolled EAP actuator", Proc. SPIE 7287, 72870G (2009).

[7] J. Fox, and N. Goulbourne, "Nonlinear dynamic characteristics of dielectric elastomer membranes", Proc. SPIE 6927, 69271P (2008).

[8] N. Huynh, G. Alici, and G. Spinks, "Force Analysis and Characterization of Polymer Actuators", Proc. IEEE/RSJ, 5465-5470 (2006).

[9] N. Bhat, and W. Kim, "Precision force and position control of an ionic polymer metal composite", Proceedings of the Institution of Mechanical Engineers, Part I: Journal of Systems and Control Engineering*,* 218(6), 421-432 (2004).

[10] K. Mallavarapu, K. Newbury, and D. Leo, "Feedback control of the bending response of ionic polymer-metal composite actuators", Proc. SPIE 4329, 301-310 (2001).

[11] Y. Fang, X. Tan, and G. Alici, "Robust adaptive control of conjugated polymer actuators", IEEE Transactions on Control Systems Technology*,* 16(4), 600-612 (2008).

[12] B. Qi, W. Lu, and B. Mattes, "Control system for conducting polymer actuators." Proc. SPIE 4695, 359-366 (2002).

[13] L. Toth, and A. Goldenberg, "Control system design for a dielectric elastomer actuator: the sensory subsystem." Proc. SPIE 4695, 323-334 (2002).

[14] N. Chuc, D. Thuy, J. Park *et al.*, "A dielectric elastomer actuator with self-sensing capability", Proc. SPIE 6927, 69270V1-7 (2008).

[15] R. Sarban, J. Oubaek, R.W. Jones, "Closed-Loop Control of a Core free rolled EAP Actuator", Proc. SPIE 7287, 72870G (2009).

[16] T. Gisby, E. Calius, S. Xie *et al.*, "An adaptive control method for dielectric elastomer devices", Proc. SPIE 6927, 69271C (2008).